

Nov 7th, 12:00 AM - Nov 8th, 12:00 AM

Influence of Fire on the Shear Capacity of Cold-Formed Steel Framed Shear Walls

M. S. Hoehler

B. Andres

Follow this and additional works at: <https://scholarsmine.mst.edu/isccss>



Part of the [Structural Engineering Commons](#)

Recommended Citation

Hoehler, M. S. and Andres, B., "Influence of Fire on the Shear Capacity of Cold-Formed Steel Framed Shear Walls" (2018). *International Specialty Conference on Cold-Formed Steel Structures*. 2.

<https://scholarsmine.mst.edu/isccss/24iccfss/session9/2>

This Article - Conference proceedings is brought to you for free and open access by Scholars' Mine. It has been accepted for inclusion in International Specialty Conference on Cold-Formed Steel Structures by an authorized administrator of Scholars' Mine. This work is protected by U. S. Copyright Law. Unauthorized use including reproduction for redistribution requires the permission of the copyright holder. For more information, please contact scholarsmine@mst.edu.

Influence of Fire on the Shear Capacity of Cold-Formed Steel Framed Shear Walls

M. S. Hoehler¹ and B. Andres²

Abstract

This paper presents experimental investigations of the performance of common lateral force-resisting systems used in cold-formed steel construction under sequential thermal (fire) and mechanical (earthquake) loading. Wall specimens with gypsum-sheet steel composite sheathing, Oriented Strand Board (OSB) sheathing, or steel strap bracing were tested. The results demonstrate that the lateral capacity of wall systems can be reduced by exposure to fire. Additionally, fire performance of wall systems can be affected by pre-damage to the fire-resistive components that provide fire protection to these walls. The results are useful for fire compartmentation design when significant lateral deformation of a building is anticipated and post-fire assessment to repair or replace a structure. The study represents a step toward developing fire fragility functions for cold-formed steel framed shear wall systems to enable performance-based fire design.

Introduction

Although extensive information exists about the structural performance and fire resistance of cold-formed steel (CFS) construction; e.g. (Schafer et al. 2016; Sultan 1996; Takeda 2003; Wang et al. 2015), there is limited knowledge about the behavior of cold-formed steel lateral force-resisting systems (CFS-LFRS) under combined hazards; in particular earthquake and fire. In 2016, a series of experiments (Phase 1) was performed at the National Fire Research Laboratory at

¹Research Structural Engineer, National Institute of Standards and Technology
matthew.hoehler@nist.gov

²PhD Student, Danish Institute of Fire and Security Technology bav@dbi-net.dk

the National Institute of Standards and Technology (NIST) to investigate the performance of earthquake-damaged gypsum-sheet steel composite panel sheathed cold-formed steel shear walls under fire load (Hoehler et al. 2017). A second phase of the project (Phase 2) extends the study to two additional levels of fire severity and two additional types of CFS-LFRS: Oriented Strand Board (OSB) sheathed and strap braced walls.

The results provide data for a range of system performance under realistic fire conditions and can inform: fire compartmentation design when significant lateral deformation of the building is anticipated, post-fire assessment to repair or replace a structure, and first responder decisions to enter a building when earthquake aftershocks are likely. The study also represents a step toward developing fire fragility functions for cold-formed steel framed shear wall systems that will enable performance-based fire design of these structures.

Test Program and Specimens

Table 1 shows the Phase 2 test matrix. Three lateral force-resisting systems were investigated: gypsum-sheet steel composite panel sheathed walls, Oriented Strand Board (OSB) sheathed walls, and steel strap braced walls. The gypsum-sheet steel composite panels were a proprietary product where the gypsum was attached to the sheet steel by adhesive. The test specimens were subjected sequentially to combinations of mechanical (cyclic shear) deformation and thermal (fire) loading to investigate their post-fire lateral behavior as well as the sensitivities of the systems to pre-fire damage. Specimen names including '01' were subjected only to load cycling to establish the baseline load-displacement response. Specimen names including '02', '03', or '04' were subjected to varied fire intensities followed by cyclic loading. Specimen names including '05' or '06' were pre-damaged with cyclic loading, subjected to fire, and then cycled to failure. The influence of pre-damage on the performance of gypsum-sheet steel composite sheathed walls was investigated in Phase 1 (Hoehler et al. 2017). Specimens with an 'R' designation were either a test replicate or a redesign of the wall.

Table 1: Phase 2 test program

Wall Type	Specimen Name	Cycling (before fire)	Loading	
			Fire	Cycling (after fire)
Gypsum-sheet steel composite	SB01	Cycle to failure	-	-
	SB02	-	Severe Parametric	Cycle to failure
	SB03	-	Mild Parametric	Cycle to failure
	SB04	-	ASTM E119 (1-hour)	Cycle to failure
Oriented Strand Board	OSB01	Cycle to failure	-	-
	OSB01R	Cycle to failure	-	-
	OSB02	-	Severe Parametric	Cycle to failure
	OSB03	-	Mild Parametric	Cycle to failure
	OSB03R	-	Mild Parametric	Cycle to failure
	OSB04	-	ASTM E119 (1-hour)	Cycle to failure
	OSB05	Drift Level 3	Mild Parametric	Cycle to failure
OSB06	Drift Level 1	Mild Parametric	Cycle to failure	
Strap braced	S01	Cycle to failure	-	-
	S01R	Cycle to failure	-	-
	S02	-	Severe Parametric	Cycle to failure
	S03	-	Mild Parametric	Cycle to failure
	S04	-	ASTM E119 (1-hour)	Cycle to failure
	S05	Drift Level 3	Mild Parametric	Cycle to failure
Additional	S06	Drift Level 1	Mild Parametric	Cycle to failure
	OSB01NG	Cycle to failure	-	-
	SB03R	-	Mild Parametric	Cycle to failure
	OSB Kitchen	-	Real furnishings	-

Each of the specimens had a length of 12 ft. (3.66 m) and height of 9 ft. (2.74 m) and was designed using Allowable Stress Design nominally following American Iron and Steel Institute (AISI) standards (*AISI S400-15 w/S1-16, North American Standard for Seismic Design of Cold-Formed Steel Structural Systems (with Supplement 1)* 2016) and (*AISI S100-16 North American Specification for the Design of Cold-Formed Steel Structural Members* 2016). Both the gypsum-sheet steel composite panel sheathed walls and the OSB sheathed walls used the framing system in Fig. 1a. The framing system for the strap braced walls is shown in Fig. 1b. The cold-formed steel framing was 6 in. (150 mm) wide, had a specified strength of 50 ksi (345 MPa), and was connected using #10 screws (4.8 mm). #8 screws (4.2 mm) spaced at 4 in. (100 mm) along the panel edges were used to attach the gypsum-sheet steel composite and OSB sheathing. The strap braced walls were designed to achieve yielding of the steel straps.

All walls were designed to achieve a 1-hour fire-resistance rating per American Society for Testing and Materials (ASTM) standard (*ASTM E119-16a Standard Test Methods for Fire Tests of Building Construction and Materials* 2016). The

cross sections are shown in Fig. 2. The design for fire-resistance of the gypsum-sheet steel composite panel sheathed walls was based on (*IAPMO-ER-1261 Sure-Board Series 200, 200W, and 200B Structural Panels Installed on Cold-Formed Steel or Wood Framed Shear Walls* 2018). The design for fire-resistance of the OSB walls was based on Underwriters Laboratory (UL) Design No. U423 (*UL Design No. 423 Fire Resistance Ratings - ANSI/UL 263 2017*) with the addition of wood panels as contemplated in (*Fire-resistance Ratings - ANSI/UL 263 2017*). The design for fire-resistance of the strap walls is based on UL Design No. U423. All walls used 5/8 in. (16 mm) thick Type X gypsum board with the joints taped and joints and fastener heads covered with one coat of joint compound on the fire-exposed side of the wall. The influence of insulation material in the wall cavity was not investigated.

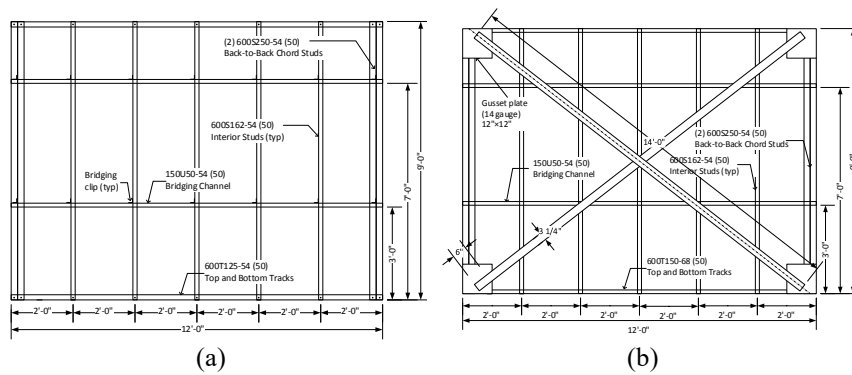


Fig. 1. Framing: (a) sheathed walls; (b) strap braced walls (1 ft. = 2.54 cm)

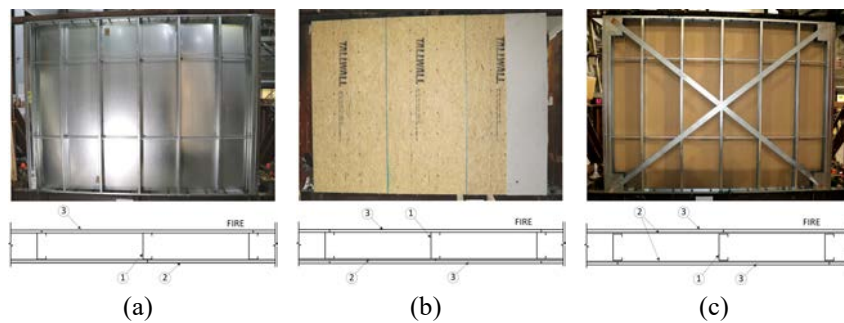


Fig. 2. Wall cross sections: (a) gypsum-sheet steel composite panel sheathed walls; (b) Oriented Strand Board sheathed walls; (c) strap braced walls (1 – steel framing; 2 – sheathing or straps; 3 – gypsum board)

Test Setup and Procedure

The test setup was informed by (*ASTM E2126-11 Standard Test Methods for Cyclic (Reversed) Load Test for Shear Resistance of Vertical Elements of the Lateral Force Resisting Systems for Buildings* 2011) but deviated as required to accommodate a burn compartment on a rolling platform. The test specimens were loaded mechanically by holding the base of the wall specimen fixed and applying a prescribed in-plane deformation to the top of the wall as shown in Fig. 3a. Out-of-plane movement of the wall was limited by four structural steel guide frames. Mechanical load was applied using a servo-hydraulically controlled actuator with a load capacity of 54 kips (240 kN) in tension and 82 kips (365 kN) in compression. Axial loading to the wall was limited to the self-weight of the specimen, actuator and top loading beam.

The thermal load was provided by a natural gas diffusion burner located in a movable compartment (interior dimensions: 9'-6" \times 11'-6" \times 4'-0" (2.9 m \times 3.2 m \times 1.2 m)). The constructed compartment is shown in Fig. 3b. The compartment was lined with two layers of 25 mm thick thermal ceramic blanket attached to sheet steel and cold-formed steel framing. The open side of the compartment that mated with the test specimen was lined with thermal ceramic blanket to provide a seal against smoke and flame leakage. The sides and top of the compartment overlapped the edges of the wall specimen approximately 3 in. (75 mm). The openings (vents) at the ends of the compartment were 5'-6" high by 4'-0" wide (1.4 m \times 1.2 m).

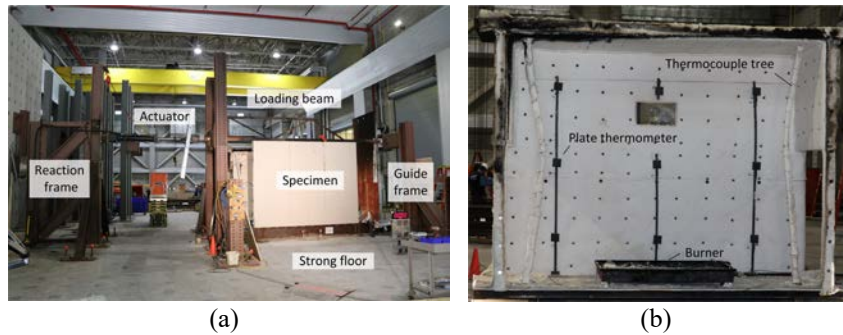


Fig. 3. Photographs of test setups: (a) mechanical loading; (b) fire loading

Mechanical Loading

ASTM E2126-11 Method C (CUREE Basic Loading Protocol) was used with reference deformations Δ of 1.5 % story drift for the sheathed walls and 2.5 % story drift for the strap braced walls. The loading procedure involves symmetric, reversed-cyclic displacement cycles grouped in phases at incrementally increasing displacement levels defined in the standard. The applied deformation was controlled using the actuator displacement. The displacement rates were selected to minimize inertial effects. With reference to Table 1, ‘cycle to failure’ was defined by a posted-peak load reduction of more than 70 % of the peak capacity. For tests with load cycling before the fire, for the sheathed walls 0.5 % and 1.5 % story drift were used for ‘Drift Level 1’ and ‘Drift Level 3’³, respectively. For the strap braced walls 0.5 % and 1.75 % story drift were used.

Fire Loading

It is assumed that the shear-resisting elements line a corridor and the fire occurs in a room adjacent to the corridor (Fig. 4). The target fire exposures were selected to represent various levels of fire severity. Three exposures were considered: (1) a 1-hour standard ASTM E119 fire curve, (2) a ‘severe’ fire exposure, and (3) a ‘mild’ fire exposure. The severe and mild fires represent realistic post-flashover compartment fire conditions with heating, fully-developed and decay phases. Fig. 5 plots the target temperature-time curves. The severity of the fire is defined in terms of exposure time and peak temperature. These values are informed by a statistical fit of data from compartment fire tests reported by (Hunt et al. 2010). Assuming a normal distribution of the compartment test data, 95 % of the reported peak compartment temperatures did not exceed 1100 °C and 50 % did not exceed 900 °C. These values were selected as the maximum temperatures for the ‘severe’ and ‘mild’ fires, respectively. Likewise, assuming a normal distribution of the duration of the fire, 70 min and 50 min represent 70 % and 50 % thresholds for the reported data, respectively. The length of the plateau was calculated using the time-to-burnout for the enclosure (τ_b) per (Hunt et al. 2010).

In multi-unit residential buildings, shear walls are commonly located along corridors adjacent to a kitchen. Assuming a kitchen compartment and taking the mean values of floor area and fuel load density reported by the National Research

³ Intermediate ‘Drift Level 2’ was not investigated.

Council Canada (Bwalya et al. 2008) for multi-family dwellings (105 sq-ft (9.8 m²) floor area with 805 MJ/m²)⁴, opening factors of 0.04 m^{0.5} and 0.09 m^{0.5} provide a time-to-burnout of 37 min and 16 min, respectively, using the Hunt et al. formulation. These times were rounded to 35 min and 15 min to define the temperature plateaus for the ‘severe’ and ‘mild’ fires. For comparison, the area under the target curve for the ‘severe’ fire represents a 20 % higher energy than ASTM E119 and the ‘mild’ fire corresponds to 40 % lower energy. The ‘mild’ fire is similar to the average upper gas layer time-temperature curves achieved in the Phase 1 tests.

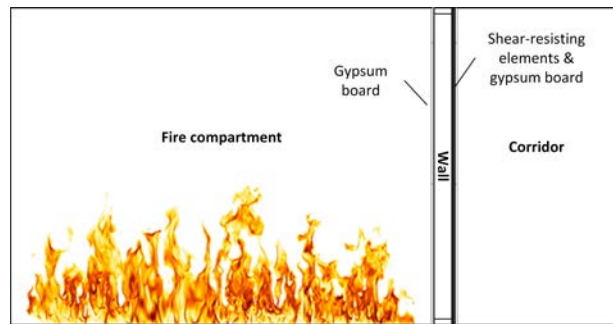


Fig. 4. Fire scenario for Phase 2 tests

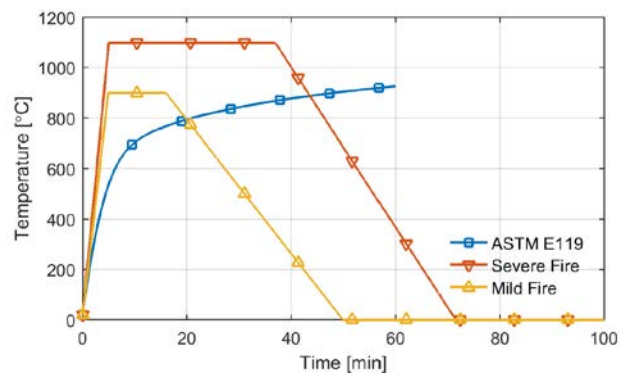


Fig. 5. Target upper layer gas temperature-time curves

⁴ Fire-related parameters are reported only in SI units because this is common practice in the U.S. and abroad.

Results

The experiments were completed immediately prior to the deadline for this paper. It is noted that the preliminary results presented here were collected from a limited series of experiments. Additional details and analysis will be included in future reports. The results presented here focus primarily on the structural, as opposed to thermal, behavior of the investigated wall systems.

The achieved upper layer gas temperatures in the compartment for the three fire scenarios investigated in Phase 2, as well as the comparable temperature measurement from Phase 1, are shown for the gypsum-sheet steel composite panel sheathed wall in Fig. 6a. The values are taken as the average of the top three sheathed, Chromel-Alumel thermocouple temperatures on the thermocouple trees at the north and south vents to the compartment (refer to Fig. 3b and Fig. 6b). The total expanded uncertainty (95 % confidence) for gas temperature measurement is estimated to be ± 2.4 % of the reading. The compartment temperatures for the OSB walls exhibited greater variability in the ASTM E119 and severe fires due to the ignition of the combustible material in the wall. Fig. 6a emphasizes that the temperature rise for the mild and severe fires, which were based on simulations of real furnishing fires, appear more rapid than that in ASTM E119 test.

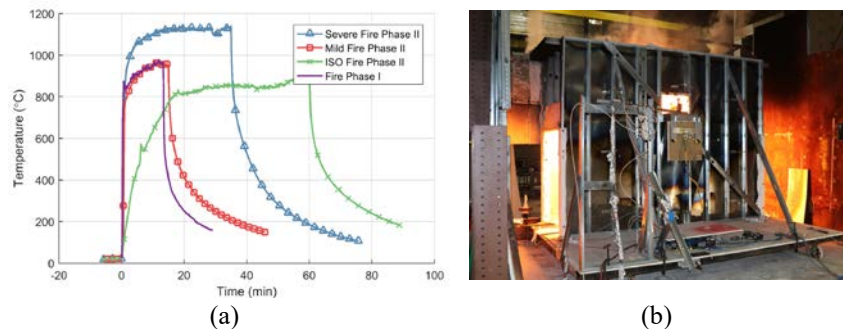


Fig. 6. (a) measured average temperature of the three top thermocouples in both trees; (b) photograph of back of compartment during fire test

Fig. 7 shows photographs of the unexposed side (opposite to the fire compartment) of the walls during the severe fires where there was no pre-damage (cycling) before the fire. Fig. 8 shows the fire-exposed side of the walls after

cooling. The gypsum-sheet steel composite panel sheathed wall exhibited charring of the paper on the unexposed gypsum at the end of the heating phase (Fig. 7a), but the sheet steel remained in place (Fig. 8a) and kept flaming combustion inside of the compartment. The Oriented Strand Board in the OSB sheathed wall ignited during the heating phase (Fig. 7b) and was largely consumed during the fire (Fig. 8b). The gypsum opposite to the compartment in the strap braced walls was breached toward the end of the heating phase (Fig. 7c), but the straps remained in place through the cooling phase (Fig. 8c). Fire-induced oxidation of the straps on the upper south side of the wall (upper left in Fig. 8c) was observed. The damage to the wall by the ASTM E119 and mild fires was less severe and is illustrated using the post-fire load-displacement response of the walls in the subsequent plots. However, for all fire sizes, the gypsum on the fire-exposed side of the walls had lost almost all its strength after the wall had cooled, effectively preventing this layer of gypsum from contributing to the post-fire mechanical behavior of the wall.

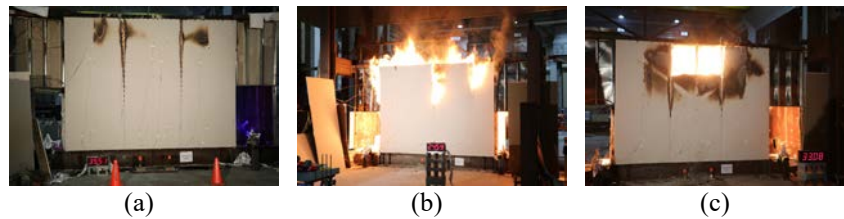


Fig. 7. Unexposed side of wall during severe fire test: (a) gypsum-sheet steel composite panel sheathed wall 35 min after ignition (end of heating); (b) Oriented Strand Board sheathed wall 25 min after ignition; (c) strap braced wall 33 min after ignition (near end of heating)

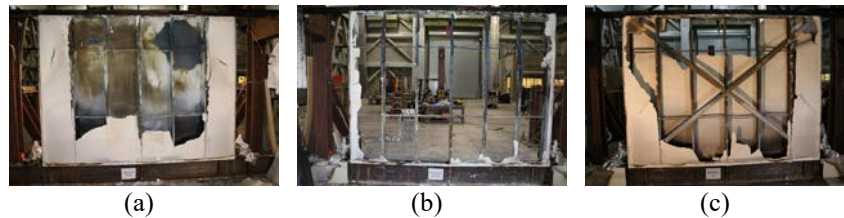


Fig. 8. Fire-exposed side of wall after severe fire test: (a) gypsum-sheet steel composite panel sheathed wall; (b) Oriented Strand Board sheathed wall; (c) strap braced wall

Fig. 9 plots the applied actuator (lateral) load versus top-of-wall drift (measured on end opposite the actuator) during mechanical loading of gypsum-sheet steel composite sheathed walls. The total expanded uncertainty (95 % confidence) associated with the force and displacement measurements are 0.36 kips (1.6 kN) and 0.09 in. (2.3 mm), respectively. In this limited set of experiments, this wall system exhibited increasingly diminished post-fire capacity with increasing fire severity. The reduction in the peak load capacity was 23 %, 58 % and 68 % for the mild, ASTM E119 and severe fire, respectively. The mild fire effectively eliminated the gypsum on the fire-exposed side of the wall and partially degraded the adhesive on the composite panels (unexposed side) which allowed buckling of the sheet steel to occur. For information on the failure mode transition see (Hoehler et al. 2017; Hoehler and Smith 2016). The ASTM E119 fire further degraded the adhesive and more widespread buckling of the sheet steel occurred. In the severe fire, the fire oxidized (burned through) several screws along the top the wall and even burned through the sheet steel at a few locations. Nevertheless, the load redistributed and the system continued to resist lateral force.

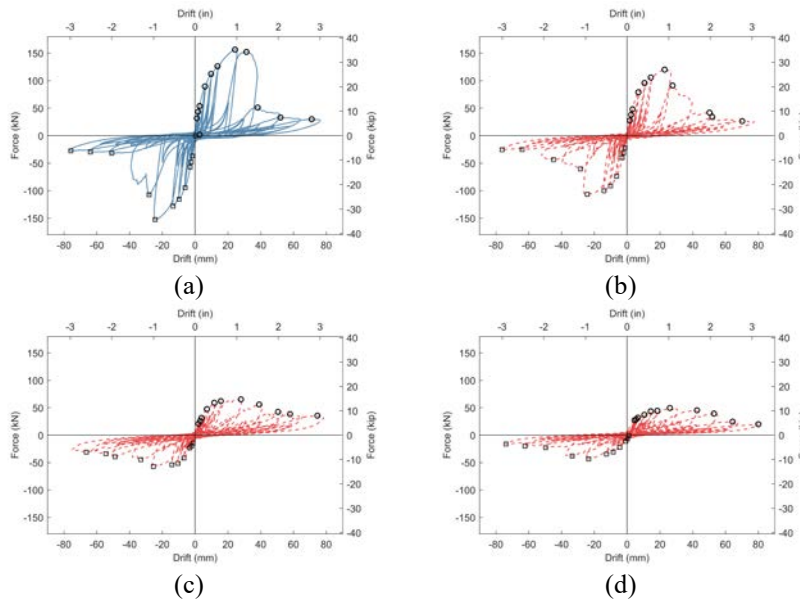


Fig. 9. Lateral load versus drift during mechanical loading of gypsum-sheet steel composite panel sheathed walls: (a) cycling without fire (SB01), (b) cycling after 'mild' fire (SB03), (c) cycling after 'E119' fire (SB04), (d) cycling after 'severe' fire (SB02)

Fig. 10 plots the lateral load versus drift during mechanical loading of OSB sheathed walls with no pre-damage prior to the fire. The investigated mild fire effectively eliminated the gypsum on the fire-exposed side of the wall and reduced the residual lateral capacity by 36 % (Fig. 10b). Both the ASTM E119 and severe fire caused the OSB to ignite. The burning was allowed to continue for 15 min after the burner was extinguished before it was suppressed with water. The reduction of the load capacity in both cases was nearly 100 % (Fig. 10c,d).

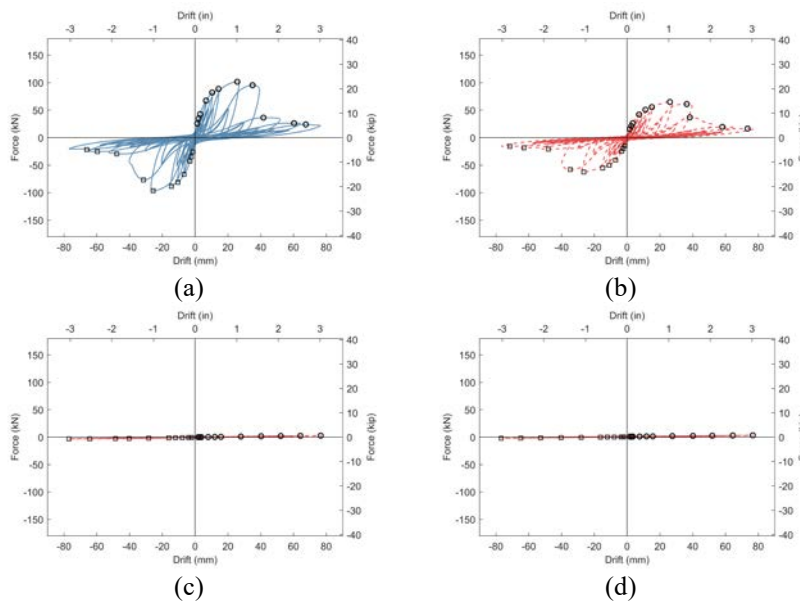


Fig. 10. Lateral load versus drift during mechanical loading of OSB sheathed walls: (a) cycling without fire (OSB01R); (b) cycling after ‘mild’ fire (OSB03); (c) cycling after ‘E119’ fire (OSB 04); (d) cycling after ‘severe’ fire (OSB02)

Cycling the wall to 0.5 % story drift prior to the fire resulted in minor damage to the skim coat on the gypsum board joints and no significant effect on the subsequent fire or post-fire cyclic performance; compare Fig. 10b to Fig. 11a. Cycling to 1.5 % story drift prior to the fire tore the tape along the joints and one of the OSB panels ignited during the mild fire. The fire was suppressed 15 min after the burner was extinguished. This burning degraded the post-fire capacity of the wall; compare Fig. 10b to Fig. 11b, however it is hard to see since the wall strength was already significantly degraded at 1.5 % drift.

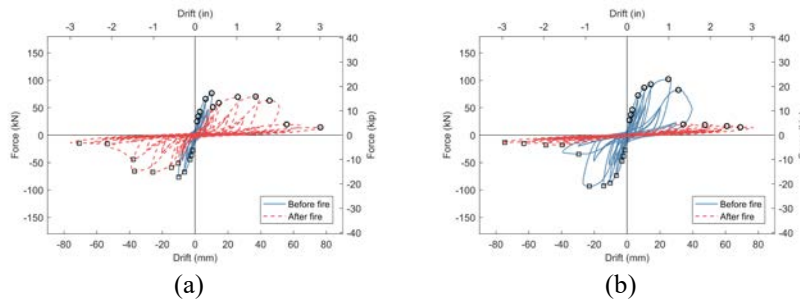


Fig. 11. Lateral load versus drift during mechanical loading of OSB sheathed walls: (a) cycling to 0.5 % drift before 'mild' fire (OSB06); (b) cycling to 1.5 % drift before 'mild' fire (OSB05)

Fig. 12 plots the lateral load versus drift during mechanical loading of steel strap braced walls with no pre-damage (cycling) prior to the fire. The baseline hysteretic behavior Fig. 12a (ambient temperature) shows a pronounced peak near maximum load followed by a long plateau as the steel straps yielded. This peak is caused by the contribution of the gypsum boards on both sides of the wall. The failure mode was rupture of the straps at the gusset plate connections and/or crippling of the chord stud just above the hold-down at large lateral displacement ($> 5\%$ story drift). The mild fire effectively eliminated the gypsum on the fire-exposed side of the wall and reduced the residual lateral capacity by 15% (Fig. 12b). This reduction appears consistent with the loss of gypsum on the fire-exposed side of the wall. The response during the ASTM E119 fire was similar to that during the mild fire, however the gypsum paper on the inside of the wall on the unexposed side was blackened indicating higher wall temperatures. The reduction to the residual capacity (17%) was similar to that during the mild fire (Fig. 12c). The severe fire burned through the gypsum on both sides of the wall toward the end of the heating phase (Fig. 7c). During subsequent cyclic loading, when cycling in the direction opposite to side where the oxidation of the straps occurred, the wall had almost zero residual load capacity (Fig. 12d, negative), while in the other loading direction close to the full ambient post-yielding load capacity was reached (Fig. 12d, positive). Interestingly, the post-fire ductility in this direction increase significantly (note axes scale change in Fig. 12d) and there was a more pronounced post-yielding hardening behavior for this limited set of tests. This appears consistent with the annealing of the cold-formed steel strap during the fire; but further study is required.

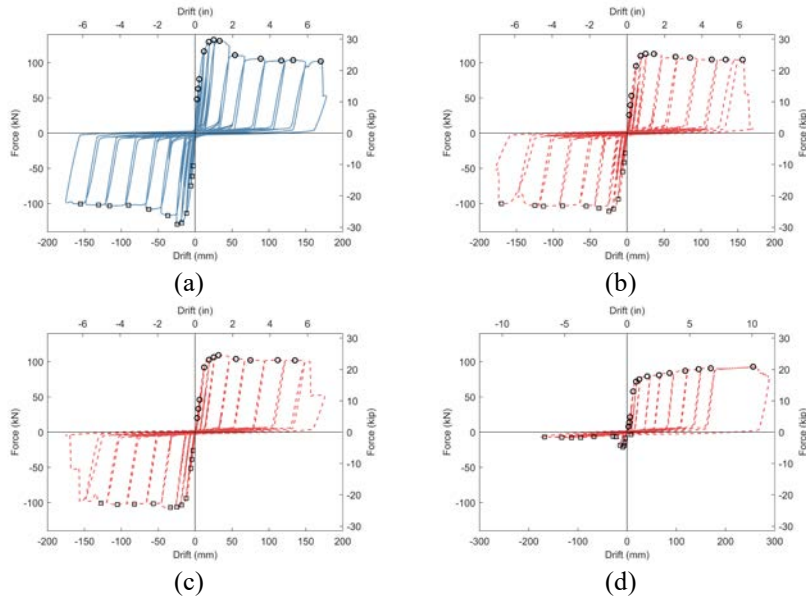


Fig. 12. Lateral load versus drift during mechanical loading of strap braced walls: (a) cycling without fire (S01R); (b) cycling after 'mild' fire (S03); (c) cycling after 'E119' fire (S04); (d) cycling after 'severe' fire (S02)

Cycling the wall to 0.5 % or 1.5 % story drift prior to the fire affected the contribution of the gypsum to the wall capacity, but had no discernable influence on the fire performance or post-fire yielding behavior (Fig. 13).

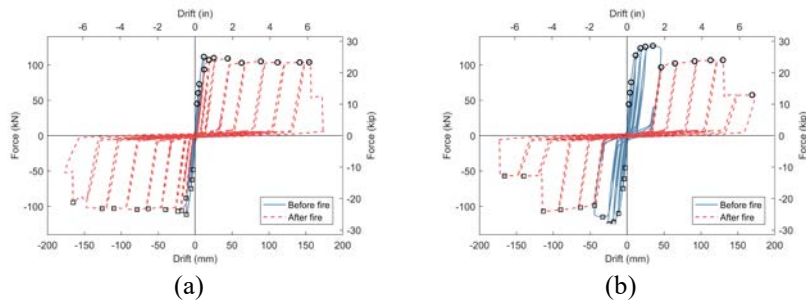


Fig. 13. Lateral load versus drift during mechanical loading of strap braced walls: (a) cycling to 0.5 % drift before 'mild' fire (S06); (b) cycling to 1.5 % drift before 'mild' fire (S05)

Conclusions

This research demonstrates an important interplay between the thermal (fire) and mechanical (cyclic) response of lateral force-resisting systems for cold-formed steel framed structures. The influence of a fire on the post-fire response differed significantly for the three investigated wall systems in this limited test series. The gypsum-sheet steel composite panel sheathing exhibited increasingly reduced post-fire capacity with increasing thermal assault. However, it maintained lateral load capacity in both loading directions even following the most severe fire investigated; allowing shear forces to redistribute even when some perimeter fasteners were burned away or the sheet steel had been comprised locally. The Phase 1 tests showed the composite panel system to be insensitive to cyclic damage prior to the fire. The strap braced walls were the most ductile and were largely insensitive to the thermal loading. However, in the case of the severe fire where a hotspot developed at a strap location, the residual lateral load capacity was reduced to essentially zero. The strap braced wall appeared to be insensitive to cyclic damage prior to the fire. For this limited set of experiments, the Oriented Strand Board (OSB) sheathed walls appeared to demonstrate a significant impact from the fire. Both the ASTM E119 and severe fires caused the gypsum-protected OSB to ignite, resulting in a total loss of residual capacity. Moreover, cycling to 1.5 % drift prior to the fire (as might occur in a major earthquake) allowed even the mild fire to penetrate the wall and ignite the OSB.

These are preliminary findings of a limited set of wall systems exposed to fire conditions. Analysis of this data is ongoing and additional testing is recommended. However, structural fire interactions such as those shown here have long gone uninvestigated and merit attention.

Acknowledgments

This work was funded by NIST. We thank Carleton Elliott (Sure-Board), Fernando Sesma (CEMCO), Jim DesLaurier (Marino/WARE), Brian Mucha (Panel Systems, Inc.), Larry Williams (SFIA), Benjamin Schafer (Johns Hopkins University), and Rob Madsen (Devco Engineering) for their expert consultation.

References

AISI S100-16 North American Specification for the Design of Cold-Formed Steel Structural Members. (2016). American Iron and Steel Institute

- (AISI), Washington, DC.
- AISI S400-15 w/S1-16, North American Standard for Seismic Design of Cold-Formed Steel Structural Systems (with Supplement 1)*. (2016). American Iron and Steel Institute (AISI), Washington, DC.
- ASTM E119-16a Standard Test Methods for Fire Tests of Building Construction and Materials*. (2016). ASTM International, West Conshohocken, PA.
- ASTM E2126-11 Standard Test Methods for Cyclic (Reversed) Load Test for Shear Resistance of Vertical Elements of the Lateral Force Resisting Systems for Buildings*. (2011). ASTM International, West Conshohocken, PA.
- Bwalya, A. C., Lougheed, G. D., Kashef, A., and Saber, H. H. (2008). *Survey Results of Combustible Contents and Floor Areas in Multi-Family Dwellings*. National Research Council Canada.
- Fire-resistance Ratings - ANSI/UL 263*. (2017). Underwriters Laboratory (UL).
- Hoehler, M. S., and Smith, C. M. (2016). *Influence of fire on the lateral load capacity of steel-sheathed cold-formed steel shear walls - report of test*. Gaithersburg, MD.
- Hoehler, M. S., Smith, C. M., Hutchinson, T. C., Wang, X., Meacham, B. J., and Kamath, P. (2017). "Behavior of steel-sheathed shear walls subjected to seismic and fire loads." *Fire Safety Journal*, 91, 524–531.
- Hunt, S. P., Cutonilli, J., and Hurley, M. (2010). *Evaluation of Enclosure Temperature Empirical Models*. Society of Fire Protection Engineers.
- IAPMO-ER-1261 Sure-Board Series 200, 200W, and 200B Structural Panels Installed on Cold-Formed Steel or Wood Framed Shear Walls*. (2018). International Association of Plumbing and Mechanical Officials (IAPMO).
- Schafer, B. W., Ayhan, D., Leng, J., Liu, P., Padilla-Llano, D., Peterman, K. D., Stehman, M., Buonopane, S. G., Eatherton, M., Madsen, R., Manley, B., Moen, C. D., Nakata, N., Rogers, C., and Yu, C. (2016). "Seismic Response and Engineering of Cold-formed Steel Framed Buildings." *Structures*, 8, 197–212.
- Sultan, M. A. (1996). "A Model for Predicting Heat Transfer through Noninsulated Unloaded Steel-Stud Gypsum Board Wall Assemblies Exposed to Fire." *Fire Technology*, 32(1), 239–257.
- Takeda, H. (2003). "A model to predict fire resistance of non-load bearing wood-stud walls." *Fire and Materials*, 27(1), 19–39.
- UL Design No. 423 Fire Resistance Ratings - ANSI/UL 263*. (2017). .
- Wang, X., Pantoli, E., Hutchinson, T. C., Restrepo, J. I., Wood, R. L., Hoehler, M. S., Grzesik, P., and Sesma, F. H. (2015). "Seismic Performance of Cold-Formed Steel Wall Systems in a Full-Scale Building." *Journal of Structural Engineering*, 141(10), 04015014.